

# A Simple Approach for Determining Contact Length between Frame and Infill of Brick Masonry Infilled R/C Frames

**Maidiawati & Thandar Oo**

*Toyohashi University of Technology, Japan*

**Y. Sanada**

*Osaka University, Japan*



## SUMMARY

This paper presents a simple approach for determining infill/frame contact length to evaluate the seismic performance of a masonry infilled R/C frame structure. The masonry infill is replaced by a diagonal compression strut, which represents distributed compression transferred diagonally between infill/frame interfaces. Infill/frame contact length can be determined by solving two equations, i.e., static equilibriums related to compression balance at infill/frame interface and lateral displacement compatibility. Consequently, strut width is presented as a function of infill/frame contact length.

An experimental verification was conducted using several brick masonry infilled R/C frames, which represented a typical R/C building with nonstructural masonry elements in Indonesia. As a result, good agreement was observed between experimental and analytical results on the performance curve of the infill including lateral stiffness and strength.

*Keywords: Infill/frame contact length, masonry wall, reinforced concrete, seismic performance, strut width*

## 1. INTRODUCTION

Reinforced concrete buildings with a masonry infill as a partition wall are used widely around the world, particularly in developing countries with high seismicity. However, the presence of a masonry infill is usually neglected in seismic design calculations of building structures, assuming it to be a nonstructural element. It has been obvious from several past studies that a masonry infill resists load and impedes deformation compatible with an infill/frame interaction. Analytical and experimental studies of the authors also showed that a masonry infill contributes significantly to the seismic performance of this kind of structure (Maidiawati et al. 2008 and 2011). The seismic performance of a masonry infill in a frame structure is commonly evaluated focusing on diagonal compression struts caused in the masonry infill. Several researchers have studied ways of modeling diagonal struts as reported by Smith and Carter (1969), El-Dakhkhni (2004) and P.G Asteris (2008). Most also focused on infill/frame contact lengths when discussing interactions between the infill and its surrounding frame. This study proposes an alternative method for determining infill/frame contact length with a simplified equation.

In this study, a masonry infill is replaced by a diagonal compression strut, which represents a distributed compression transferred diagonally between infill/frame interfaces. The infill/frame contact length can be determined by solving two equations, i.e., static equilibriums related to the compression balance at infill/frame interface and lateral displacement compatibility. Consequently, the equivalent strut width is presented as a function of infill/frame contact length.

A series of structural tests was conducted to verify the validity of the proposed method. Experimental specimens included several Indonesian brick masonry infilled frames of different thicknesses and configurations of infill. The specimens represented a typical R/C building with nonstructural masonry elements in Indonesia, which was an earthquake-damaged building investigated by the authors after the 2007 Sumatra earthquakes (Maidiawati and Sanada 2008). This paper compares experimental results and numerical simulations using the proposed method.

## 2. ANALYTICAL MODEL OF MASONRY INFILLED FRAMES

This study targets a brick masonry infilled R/C one-bay frame with a fixed base and a rigid beam, as shown in Figure 1a, representing a multi-story infilled frame where beam flexural deformation is constrained by the infill. Contact/separation is caused between the bounding column and infill under column flexural deformation and infill shear deformation, as shown in Figure 1a. In this study, contact length between column and infill was derived as follows.

The masonry infill wall was replaced by a diagonal compression strut having the same thickness and material properties as the infill panel. In this model, however, a compression stress block at the infill/frame interface was replaced by an equivalent rectangular block, as shown in Figure 1b, where the averaged compressive strength,  $f_m'$ , was given for the infill strength.  $f_m'$  was evaluated by multiplying the uniaxial compressive strength of infill,  $f_m$ , by a reduction factor,  $\alpha$ , which resulted in a value of approximately 0.65 in the calculations described below. As a result, the compression strut was represented by a force that was distributed uniformly symmetrically along the diagonal axis of the infill. The lateral distribution force along the column height, which acts on the bottom of the compressive column, is given by Eq. 2.1.

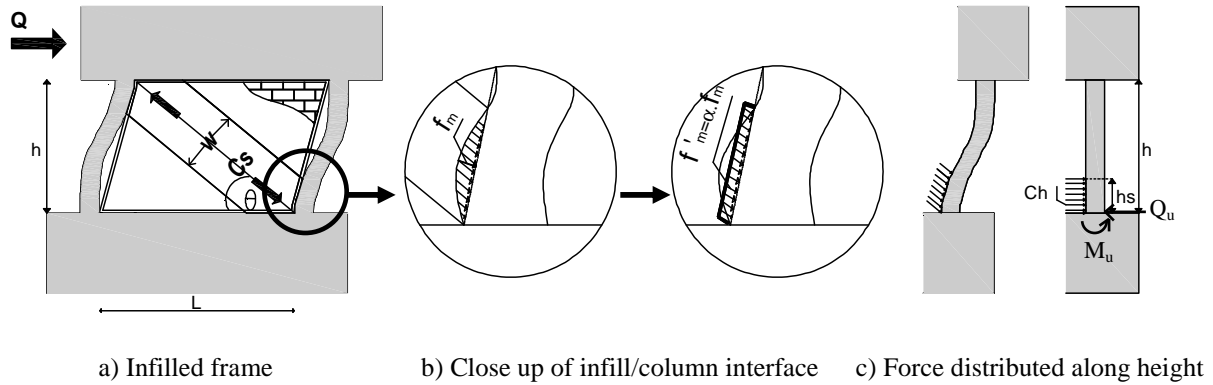


**Figure 1.** Modeling of masonry-infilled frame

$$C_h = t f_m' \cos^2 \theta \quad (2.1)$$

where,  $C_h$ : uniformly distributed force along column height, as shown in Figure 1c,  $t$ : thickness of infill,  $\theta$ : inclination angle of strut, as shown in Figure 1a.

Assuming that the column on the compressive side (right side in Figure 1a) yields in flexure at the bottom, the moment distribution along column height,  ${}_cM(y)$ , is obtained with Eq. 2.2. Yield moment, however, is calculated with Eq. 2.3 based on the JBDPA standard (2005).

In the case of  $0 \leq y \leq h_s$

$${}_cM(y) = {}_{y=0}M_u - Q_u y + 1/2 C_h y^2 \quad (2.2a)$$

In the case of  $h_s \leq y \leq h$

$${}_cM(y) = {}_{y=0}M_u - Q_u y + C_h h_s y - 1/2 C_h h_s^2 \quad (2.2b)$$

$$M_u = 0.8 a_t \sigma_y D + 0.5 N D \left( 1 - \frac{N}{b D F_c} \right) \quad (2.3)$$

where,  $h_s$ : infill/column contact height, as shown in Figure 1c,  $h$ : column height, as shown in Figure 1c,

$M_u$ : flexural strength of column,  $Q_u$ : shear force at column bottom, which is determined with Eq. 2.5,  $a_t$ : total cross-sectional area of tensile reinforcing bars,  $\sigma_y$ : yield stress of longitudinal reinforcement,  $D$ : column depth,  $N$ : axial force,  $b$ : column width,  $F_c$ : compressive strength of concrete. However, the axial force at the bottom of the column was calculated as a summation of building weight (initial axial load),  $N_a$ , axial force due to shearing force in the beam,  $N_b$ , and vertical component of the strut force,  $C_v h_s (= t f_m' \cos \theta \sin \theta h_s)$ , as shown in Figure 2.

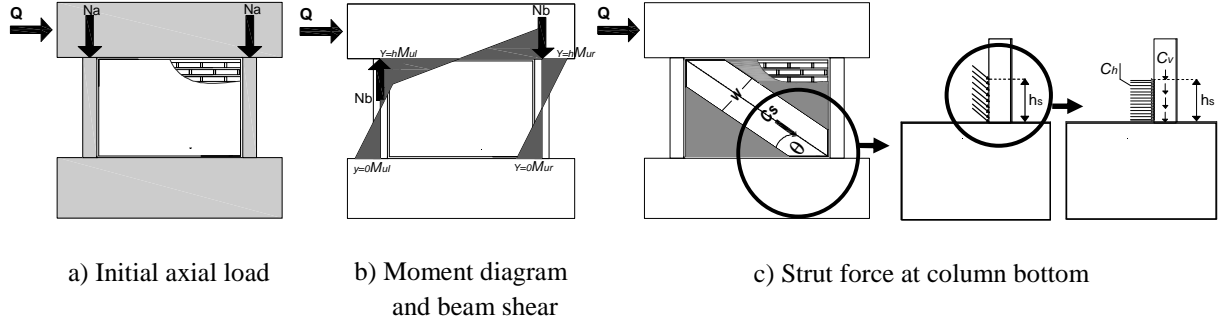


**Figure 2.** How to evaluate axial force at column bottom

Lateral displacement along column height,  ${}_c\delta(y)$ , is produced by double integrals of Eq. 2.2, which is shown by Eq. 2.4.

In the case of  $0 \leq y \leq h_s$

$${}_c\delta(y) = \frac{1}{EI} (1/2 M_u y^2 - 1/6 Q_u y^3 + 1/24 C_h y^4) \quad (2.4a)$$

In the case of  $h_s \leq y \leq h$

$${}_c\delta(y) = \frac{1}{EI} (1/2 M_u y^2 - 1/6 Q_u y^3 + 1/6 C_h h_s y^3 - 1/4 C_h h_s^2 y^2 + 1/6 C_h h_s^3 y - 1/24 C_h h_s^4) \quad (2.4b)$$

where,  $EI$ : bending stiffness.

In Eqs. 2.2 and 2.4,  $Q_u$  is given by Eq. 2.5 when assuming a rotation of zero at the column top.

$$Q_u = \frac{2M_u}{h} + C_h h_s - \frac{C_h h_s^2}{h} + \frac{C_h h_s^3}{3h^2} \quad (2.5)$$

On the other hand, lateral deformation along infill height,  ${}_i\delta(y)$ , is defined by Eq. 2.6, assuming uniform shear strain,  ${}_i\theta$ . Therefore, intersection height between column and infill can be evaluated by solving Eq. 2.7, as shown in Figure 3. The figure shows that intersection height should equal  $h_s$ . The unknown  $h_s$  was obtained iteratively after satisfying Eq. 2.7. In this study, the Newton Raphson method was used to find  $h_s$ . The procedure above is presented in the flowchart in Figure 4.

$${}_i\delta(y) = {}_i\theta y = \frac{{}_c\delta(y=h)}{h} y \quad (2.6)$$

$${}_c\delta(h_s) = {}_i\delta(h_s) \quad (2.7)$$

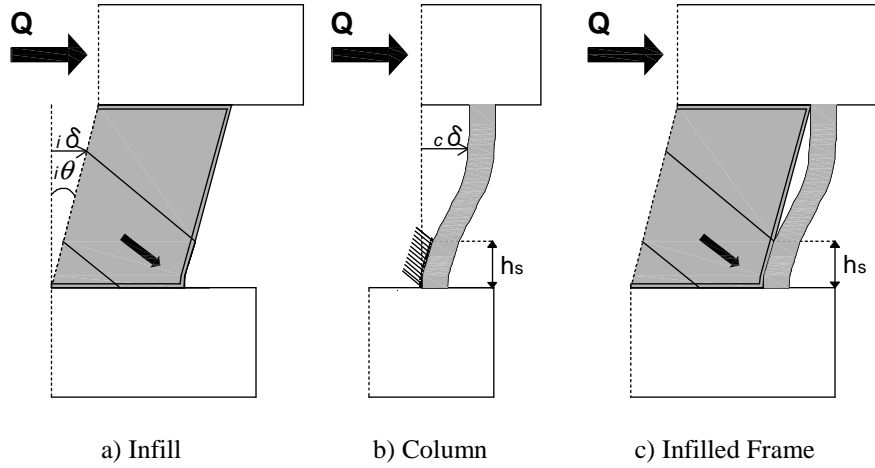


**Figure 3.** Lateral displacement compatibility along column height

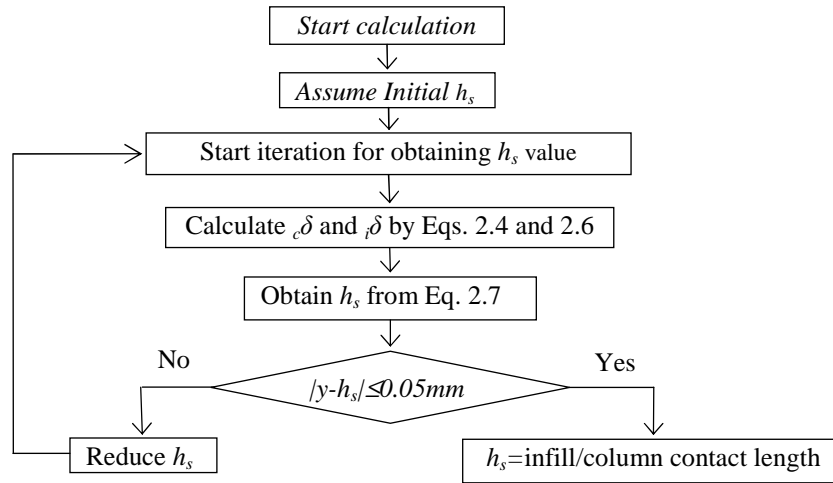


**Figure 4.** Flowchart for identifying infill/column contact length

The width of compression strut, which is shown in Figure 1, is determined as a function of infill/column contact height by Eq. 2.8.

$$w = 2h_s \cos \theta \quad (2.8)$$

### 3. EXPERIMENT FOR VERIFICATION

To clarify the validity of the proposed method experimentally, a series of structural tests was conducted on R/C frames with/without a brick masonry infill. The specimens represented a partial frame of a typical R/C building, as shown in Photo 1 and Figure 5, which was investigated in detail by the authors after the 2007 Sumatra earthquakes, Indonesia (Maidiawati and Sanada 2008). The following experimental program and results have been partially reported in Maidiawati et al. (2011) with the exception of two specimens with infill consisting of scaled bricks.





**Photo 2.** Preparation of brick wall specimen



**Photo 3.** Installation of brick wall

### 3.1.3. IF\_SBw/oFM and IF\_SB Specimens

IF\_SBw/oFM and IF\_SB specimens had a scaled brick infill consisting of 1/2.5 scale bricks having dimensions of 88 mm in length, 44 mm in width and 20 mm in height. Although the compressive strength of the scaled bricks made in Japan was arranged to be similar to that of Indonesian bricks, the masonry prisms with mortar beds exhibited higher strengths for IF\_SBw/oFM and IF\_SB specimens from material tests, as shown in Table 3.2. Bricks were laid up in the interior clear height of frames with mortar beds at a volume ratio of cement: sand: water = 1: 4: 1.4. Finishing mortar with a thickness of 8 mm was applied only to the wall surfaces of IF\_SB specimen, which resulted in an infill thickness of 44 mm and 60 mm for IF\_SBw/oFM and IF\_SB, respectively. Figure 7 is a detailed drawing of the IF\_SB specimen.

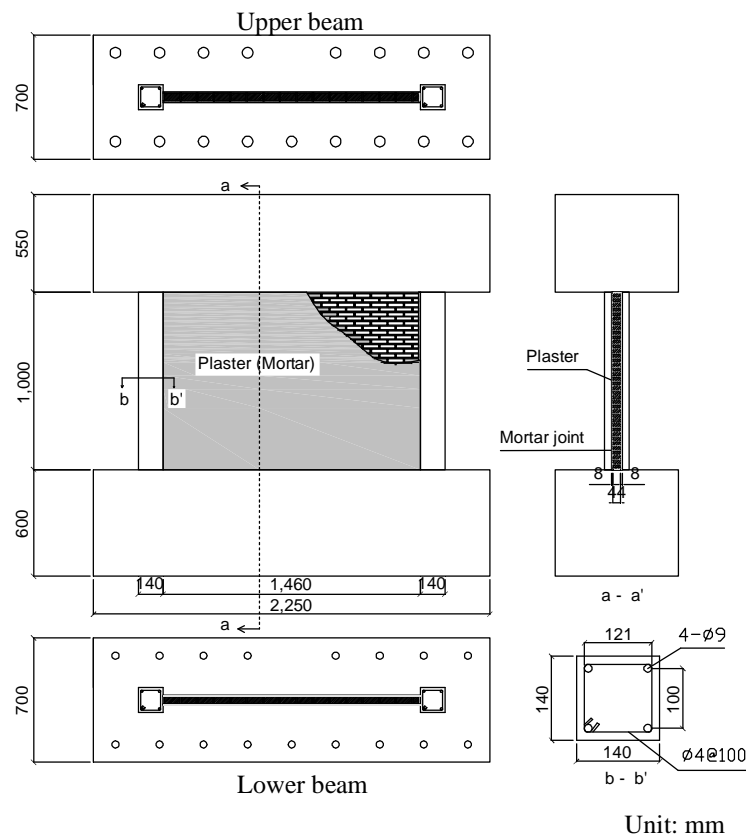


**Figure 7.** Detailed drawing of IF\_SB specimen

**Table 3.1.** Parameters for specimens

Specimens	Column	Experimental parameters	
		Brick wall	Plaster
BF	cross-section: 140x140 main bar: 4-Ø9 hoop: 2- Ø4@100	none	none
IF_FB		thickness: 100 mm	20 mm (each side)
IF_SBw/oFM		thickness: 44 mm	none
IF_SB		thickness: 44 mm.	8 mm (each side)

**Table 3.2.** Material properties

<b>Concrete</b>			
Specimen	Material age	Compressive strength	Tensile strength
	Day	N/mm <sup>2</sup>	N/mm <sup>2</sup>
BF	44	19.6	1.89
IF_FB	37	20.6	1.96
IF_SBw/oFM	63	26.6	1.90
IF_SB	67	27.3	1.98
<b>Mortar</b>			
Specimen	Material age	Compressive strength	Tensile strength
	Day	N/mm <sup>2</sup>	N/mm <sup>2</sup>
IF_FB (only for boundaries)	42	40.8	3.33
IF_SBw/oFM	42	44.7	2.33
IF_SB	46 for infill 44 for finishing	48.6 for infill 42.9 for finishing	3.26 for infill 2.89 for finishing
<b>Masonry prism</b>			
Specimen	Material age	Compressive strength ( $f_m$ )	Young's modulus ( $750*0.65f_m$ )
	Day	N/mm <sup>2</sup>	N/mm <sup>2</sup>
IF_FB	Unknown	2.91	1418.6
IF_SBw/oFM	42	16.3	7946.3
IF_SB	46	18.5	9033.4
<b>Reinforcing bar</b>			
Bar number	Yield strength	Tensile strength	
	N/mm <sup>2</sup>	N/mm <sup>2</sup>	
9 (BF, IF_FB)	355	440	
4 (BF, IF_FB)	583	631	
9 (IF_SBw/oFM, IF_SB)	338	382	
4 (IF_SBw/oFM, IF_SB)	497	778	

### 3.2. Test Methods

The specimens were subjected to a constant vertical load of 183.4 kN ( $\approx 0.24 \times$  column sectional area  $\times$  compressive strength of concrete) based on the estimated weight of the upper floors. Then, reversed cyclic lateral loads were applied to the specimens. Incremental loads were controlled by drift angle,  $R$  (rad.), ratio of lateral displacement to column height. The lateral loading program had an initial cycle to  $R=1/800$  followed by two cycles to  $R=1/400$ ,  $1/200$ ,  $1/100$ ,  $1/50$ ,  $1/25$  and  $1/12.5$  for BF and IF\_FB specimens, and an initial cycle to  $R=1/400$  followed by two cycles to  $R=1/200$ ,  $1/100$ ,  $1/50$ ,  $1/25$  and  $1/12.5$  for IF\_SBw/oFM and IF\_SB specimens, respectively. When the specimens failed, loading was stopped. The schematic representation of the experimental set-up and the lateral loading history are shown in Figures 8 and 9, respectively. The shear span to depth ratio ( $= h_w/l_w$  illustrated in Figure 8) of the specimens was maintained at 0.75 throughout the tests so that lateral loads were applied at an assumed second floor height of 1200 mm.

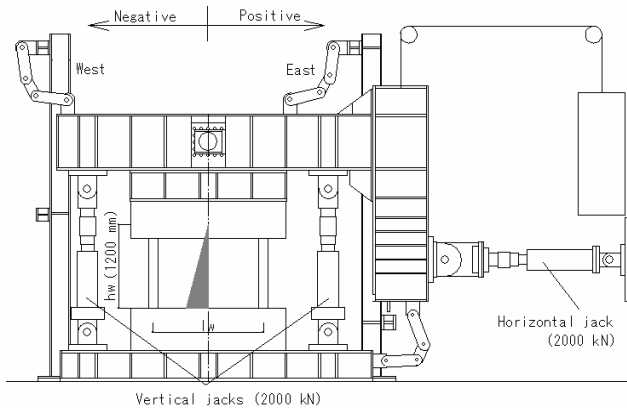


Figure 8. Schematic view of test set-up

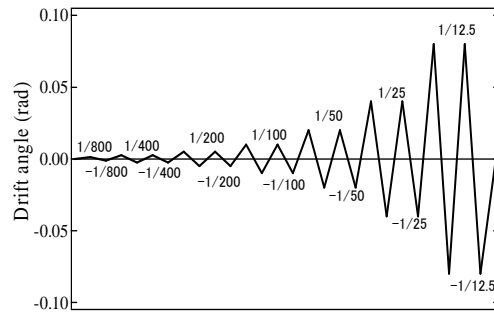


Figure 9. Lateral loading history for BF and IF\_FB

### 3.3. Test Results and Discussion

Figure 10 compares lateral force vs. drift ratio,  $R$ , relationships between the specimens. The maximum lateral strength of 36.8 kN was observed at 2.0% for the BF specimen. On the other hand, the maximum strengths reached 174.0 kN, 174.75 kN and 257.25 kN at 0.5%, 0.25% and 0.23% drift ratios for IF\_FB, IF\_SBw/oFM, and IF\_SB, respectively. The deformation capacity, which was defined as a deformation where post-peak strength dropped to 80% of peak strength, was 2.8% for BF, whereas they decreased to 1.6%, 1.0% and 0.5% for IF\_FB, IF\_SBw/oFM, and IF\_SB, respectively.

The infill contribution was extracted by evaluating the difference between lateral forces of infilled frame and bare frame at each load step (at the same drift ratio), as shown in Figure 11. In this study, the envelope curves were simulated according to the proposed analytical method as follows.

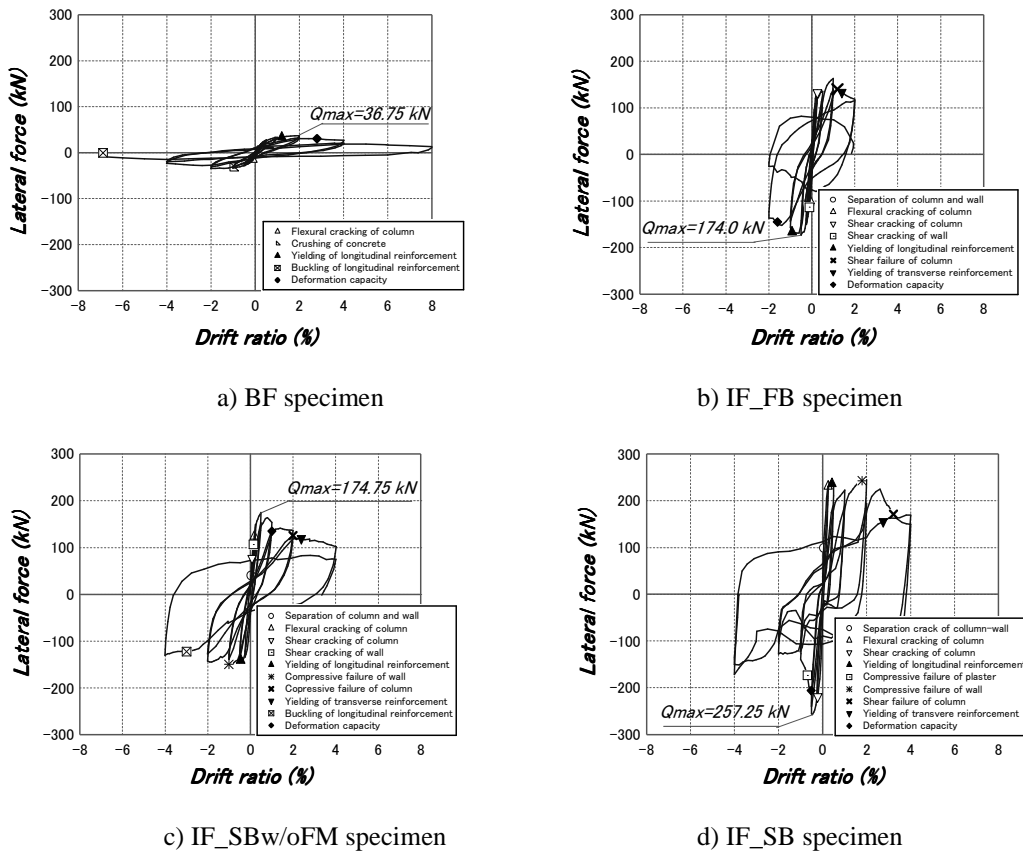


Figure 10. Lateral force–drift ratio relationships of infilled frames

#### 4. VERIFICATION OF ANALITICAL MODEL

According to the analytical method proposed in this study, infill/frame contact lengths,  $h_s$ , were evaluated to be 312 mm, 259 mm, and 218 mm for IF\_FB, IF\_SBw/oFM and IF\_SB, respectively. The envelopes of the performance curves of the infill, as shown in Figure 11, were evaluated based on the strut widths obtained by Eq. 2.8. Equations 4.1 and 4.2 give initial lateral stiffness,  $K$ , and ultimate lateral strength,  $Q$ , of the compression strut replacing the infill, respectively.

$$K = \frac{E_m w t}{d} \cos^2 \theta \quad (4.1)$$

$$Q = C_s \cos \theta = w t f'_m \cos \theta \quad (4.2)$$

where,  $E_m$ : elastic modulus of infill ( $= 750 f'_m$ ) based on Paulay and Priestley (1991), and  $d$ : diagonal length of frame.

The evaluated lateral stiffness and strength of infill are compared to the experimental results in Figure 11. Good agreement was obtained between experimental and analytical results until strength began to drop after peaking. It was verified that the proposed method could be used reasonably for estimating the seismic performance of a masonry infill.

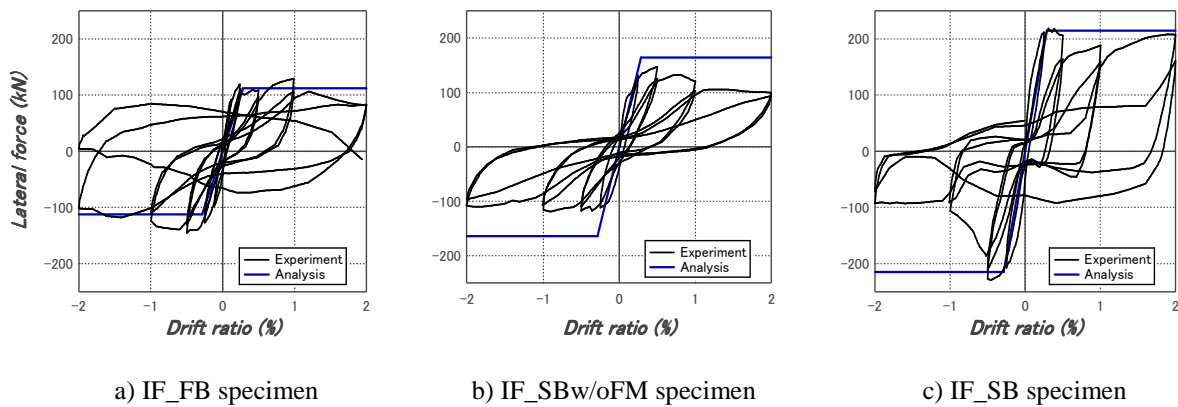


**Figure 11.** Lateral Force-drift ratio relationship of infill

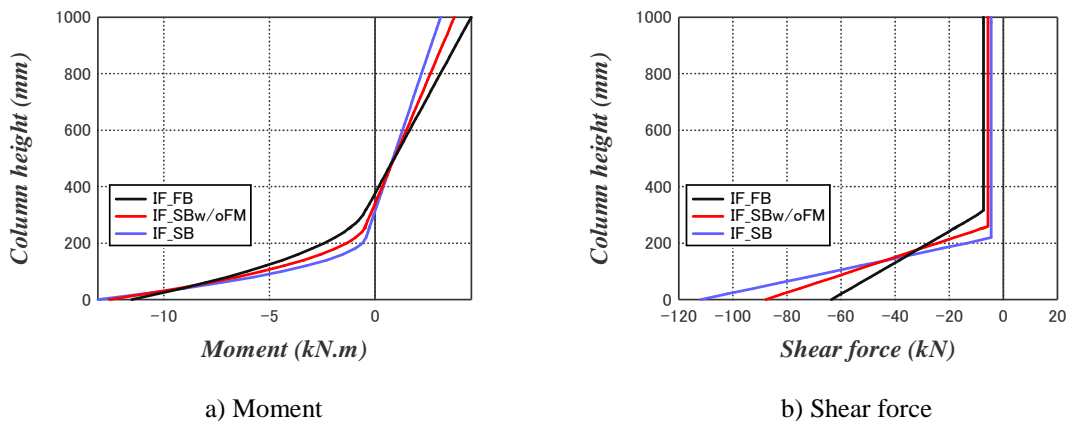


**Figure 12.** Stress diagrams of column

Moreover, the proposed method can identify distributions of bending moment and shear force along the column height, as shown in Figure 12. Bending moments at the base of the column were 11.5 kN.m, 12.6 kN.m and 13.1 kN.m for IF\_FB, IF\_SBw/oMF and IF\_SB, respectively. Shear forces at

the column bottom were 63.6 kN, 87.8 kN and 111.9 kN for IF\_FB, IF\_SBw/oMF and IF\_SB, respectively. Compared to the moment of 10.5 kN.m and shear force of 21.0 kN for BF, it was found that the masonry infill increased not only the strength of the overall frame, but also local bending moment and shear force acting on the column. Therefore, the deformation capacities of infilled frame specimens were much lower than that of the bare frame specimen.

## 5. CONCLUSIONS

The following conclusions were obtained from analytical and experimental studies on R/C frames with brick masonry infill.

1. A simplified analytical method was proposed to evaluate infill contribution to the seismic performance of masonry infilled RC frames, and was verified through a series of structural tests. An infill panel is replaced by a diagonal compression strut in the proposed analytical method.
2. Contact length between column and infill was evaluated based on the compression balance at the infilled/frame interface and lateral displacement compatibility under column flexural and infill shear deformations. Compression strut width was determined with evaluated contact length.
3. The performance curve of the infill in the experimental specimens was simulated by the proposed method. Consequently, good agreement was observed between experimental and analytical results.
4. An infill can increase local bending moment and shear force at bounding columns, which seemed to decrease the deformation capacities of bounding columns.

## ACKNOWLEDGEMENT

This study was supported financially by Housing Research Foundation (Jusoken), Japan, Indonesian Ministry of Higher Education, and Japan Ministry of Education, Culture, Sports, Science and Technology (MEXT).

## REFERENCES

- B. Stafford Smith, Carter CA (1969). A Method of Analysis for Infilled Frames. Proc. ICE., pp. 44: 31-48.
- P.G. Asteris. (2008). Finite Element Micro-Modeling of Infilled Frames. *Electric Journal of Structural Engineering* **8**.
- Maidiawati and Sanada Y. (2008). Investigation and Analysis of Buildings Damaged during the September 2007 Sumatra, Indonesia Earthquakes. *Journal of Asian Architecture and Building Engineering* **7:2**,371–378.
- Maidiawati, Sanada Y, Daisuke Konishi, and Jafril Tanjung. (2011). Seismic Performance of Nonstructural Brick Walls Used in Indonesian R/C Buildings. *Journal of Asian Architecture and Building Engineering* **10:1**,203-210.
- The Japan Building Disaster Prevention Association (JBDPA). (2005). English Version, 1<sup>st</sup>, Standard for Seismic Evaluation of Existing Reinforced Concrete Buildings, 2001.
- T. Paulay, M.J.N. Priestley. (1991). Seismic Design of Reinforced Concrete and Masonry Buildings, ISBN 0-471-54915-0.
- Wael W. El-Dakhkhni, Ahmad. Hamid and Mohamed Elgaaly. (2004). Strength and Stiffness Prediction of Masonry Infill Panels. *13<sup>th</sup> World Conference on earthquake Engineering Vancouver*, B.C., Canada.